

# FLAME VISIBILITY IN HYDROGEN APPLIANCES

Douglas Proud<sup>1</sup>, Adam Gee<sup>1</sup>, Michael Evans<sup>2</sup>, Neil Smith<sup>1</sup>, Paul Medwell<sup>1</sup>

<sup>1</sup>The University of Adelaide, Australia

<sup>2</sup>University of South Australia, Australia

## ABSTRACT

One of the benefits of the direct use of hydrogen is its ability to be burned in a similar way to natural gas, using appliances with which the community is already familiar. This is particularly true for applications where electrification is neither practicable nor desirable. One common example is domestic cooking stoves, where the open flame offers numerous real and perceived benefits to the chef. Similarly, many commercial and industrial appliances rely on the unique properties of combustion to achieve a desired purpose that cannot readily be replaced by an alternative to an open flame.

Despite the enormous decarbonisation potential of the direct replacement of natural gas with hydrogen, there are some operational constraints due to the different burning characteristics of hydrogen. One of the challenges is the low visible light emission from hydrogen flames. The change in visible radiation from the combustion of hydrogen compared with natural gas is a safety concern, whereby visual observation of a flame may be difficult. This paper aims to provide clarity on the visual appearance of hydrogen flames via a series of measurements of flame visibility and emission spectra, accompanied by the assessment of strategies to improve the safe use of hydrogen.

## 1. INTRODUCTION

### 1.1 Background and Motivation

The important role of hydrogen as a renewable source of energy is widely understood [1]. Not only can hydrogen be used to power fuel cells to generate electricity, it can also be used directly as a fuel in combustion applications, ranging from domestic appliances to large-scale industrial installations [2, 3]. One particular area in which hydrogen is well-positioned to displace fossil fuels is in existing gas networks [4]. The addition of hydrogen to natural gas pipelines in relatively low proportions has been trialled and successfully implemented in several networks globally, and studies indicate that most pipelines can accommodate addition of hydrogen up to at least 10% (by volume), with only slight modifications to the distribution system required [5]. Ultimately, the aim is to extend this to achieve a zero-carbon gas pipeline of 100% hydrogen, which can be used as a fuel for combustion appliances and to power fuel cells. There are, however, a number of safety concerns which must be addressed when implementing hydrogen as a fuel source, particularly with regards to pure or near-pure hydrogen.

From an end-use perspective, a challenge associated with the use of 100% hydrogen as a fuel source is the lack of a clearly visible flame [6]. The lack of a visible flame can present a hazard both from the user not being aware of when the flame is lit, and equally, being unaware when the flame is extinguished. In the context of a kitchen cooktop burner, for example, an “invisible flame” would present an obvious burn hazard when lit, particularly for users who are accustomed to a conventional natural gas cooktop. Such a flame would also present an increased risk of a dangerous build-up of gas, since the user would be more likely to leave the gas turned on following the accidental extinguishing of the flame. This latter concern is partially addressed by the fact that modern cooktops typically feature some form of flame supervision device which is interlocked with the gas supply to shut-off the gas flow in the case of the flame being extinguished. However, it should be noted that these systems are intended to be used as a back-up feature, and tend to involve a significant delay prior to activation of the shut-off valve. A potential option to enable a cooktop burner to be safely operated without a visible flame is to provide an alternative method of flame supervision, which is coupled with a flame indicator (e.g. an LED light), such that the user can determine if the flame is extinguished without a significant delay, although this would incur additional costs to be passed on to appliance manufacturers and hence consumers.

The lack of a visible flame also has implications from a user-friendliness and social acceptance perspective. For example, it is common for end-users to determine their required heat input or turn-down settings based on the visual appearance of the flame(s) for both gas cooktops and gas fires [7]. Again, a potential work-around could be in the form of a separate visual indicator to gauge the input settings; however, to maximise the social acceptance of hydrogen in domestic settings, it would be desirable to maintain a similar behaviour to that of existing natural gas appliances.

The current study is focussed on assessing the feasibility of improving the safety and performance of hydrogen as a fuel via the addition of a small amount of a hydrocarbon, herein referred to as a dopant. Experimental results based on toluene as a dopant are presented, including flame photography for various burners and lighting conditions, and spectral measurements. Other potential benefits of doping with such a fuel include improved radiative heat transfer characteristics and the ability to detect leaks via olfactory detection [8-10], although these topics are outside the scope of the current report.

## 1.2 Light Emissions from Pure Hydrogen Flames

It is widely known that flames resulting from pure hydrogen combustion in air typically produce low levels of visible radiation, compared with the conventional combustion of hydrocarbons [6, 11]. A common misconception, however, is that hydrogen flames are invisible. A faint blue colour has consistently been observed under low-light conditions [6, 12], as well as a red “tail” to the flame in some cases [6, 13]. Some early sources claim that the only source of visible emissions in pure hydrogen-air flames is that which stems from the hydroxyl (OH) bands, which are primarily in the UV but have slight overlap in the blue end of the visible spectrum [11, 14]. The presence of additional radiation has often been attributed to impurities, including sodium, calcium and sulphur [11]. To examine the impact of impurities, hydrogen at both 99% and 99.999% purity has been tested [6], and no discernible difference in the flame spectrum was observed. Additionally, pure oxygen mixed with argon was used as the “air” mixture, and once again there was no effect. With impurities ruled out, the reddish appearance of these flames is attributed to the vibrational excitation of water molecules within the flame. As reported by Schefer et al. [6], the reddish colour observed was faint, with the flames clearly visible only under reduced-light conditions. This behaviour is expected, since the excitation of water molecules results in relatively low emissions of light in the visible region, with peaks in the near infra-red [12]. Other experiments and trials, however, have reported a relatively strong orange appearance of hydrogen flames, such that the flames are visible even under well-lit conditions.

The presence of this relatively bright “orange” colour is largely attributed to the presence of impurities. One suggestion is that these impurities stem from hydrogen embrittlement during storage/transportation, which leads to the presence of metallic particles within the fuel stream [12]. This was supported by experiments performed with and without a 0.5- $\mu\text{m}$  filter installed on the fuel line, which showed a statistically significant reduction in intensity. Electron microscopy revealed the presence of iron, sodium and calcium in the fuel stream. While these results show that the colour is at least partially related to the presence of filterable particles in the hydrogen, it does not confirm that the particles which produce this colour stem from embrittlement. It is also worth mentioning that sodium impurities from the ambient air have been found to contribute to the emission spectra in previous flame spectroscopy studies [15, 16], with a strong peak at 589 nm which corresponds to a distinctive orange colour. The effect of impurities in the context of the current investigation is further discussed in Section 3.1.

It should be noted that, although visible emissions can be detected from hydrogen flames, the intensity of these emissions is in general much lower than comparable hydrocarbon flames. While some studies indicate that impurities could lead to a flame of similar visibility to natural gas, it is not clear if this can be relied upon to produce a consistently observable flame in all situations. Since domestic appliances involving an open hydrogen flame would typically be operated in a well-lit environment (e.g. a kitchen stovetop), the visibility of a hydrogen flame should also be assessed with this in consideration. Ultimately, for hydrogen to be safely used in appliances, the visibility achieved must be similar to or greater than that of a natural gas flame, particularly when taking into account the increased flammability of hydrogen and therefore the elevated risks associated with leaks.

### 1.3 Improving Visibility of Hydrogen Flames

To improve the efficiency of gas-fired furnaces, the addition of metal oxide nanoparticles to increase radiative heat transfer in flames has been investigated [17]. It was found that the addition of inert alumina particles to LPG fuel leads to a significant increase in flame luminosity and a larger visible flame area. For domestic applications, it would likely be more practical to introduce dopants that do not involve particulates (e.g. PM2.5) [7]. Additionally, the use of particles would not be compatible with injection throughout the gas network, since it would either form deposits in the pipeline or be filtered out at various points throughout the network [18].

The addition of hydrocarbons in relatively low proportions—herein referred to as “doping”—is another method of increasing the visibility of hydrogen flames. In conventional hydrocarbon fuels, much of the radiative flux—and therefore much of the visible light—stems from soot particles, which produce high levels of broadband radiation in a flame [19]. Due to the importance of soot formation in applications such as furnaces, along with the need to suppress it in other devices such as gas turbines, the physical and chemical processes relating to soot formation have been studied in depth over the years. The tendency to form soot varies greatly depending on the initial fuel composition, and a useful method of comparing and quantifying the sooting propensity of different fuels is through the Yield Sooting Index (YSI) [20]. This index is based on measurements of the soot volume fraction in methane flames doped with 400 ppm of the hydrocarbon of interest. In general, it is understood that aromatic hydrocarbons, such as toluene, tend to have relatively high YSIs due to the presence of a benzene ring and the associated high carbon-to-hydrogen ratio [21]. By selecting dopants with high YSIs, there is potential to significantly enhance the visibility of hydrogen flames, even at very low concentrations of dopant.

Another attractive feature of using high YSI hydrocarbon fuels as a dopant for hydrogen flames is the fact that these fuels typically exist in the liquid state at standard conditions [20]. This offers a range of benefits over gaseous additives in terms of transportation and storage, since pressurisation is not necessary and leak prevention is less problematic. This makes it feasible to inject the dopant much closer to the end use side, or even within the plumbing configuration of individual appliances, allowing pure hydrogen to still be used for other applications, such as in fuel cells. Additionally, if the dopant were to be injected into the pipeline as a vapour upstream of a fuel cell, the relatively high boiling point would enable it to be separated from hydrogen via a condenser.

## 2. METHODOLOGY

### 2.1 Experimental Overview

For the experimental investigation in this project, the focus is on the feasibility of using toluene as a dopant. Toluene was selected primarily due to its very high sooting propensity which has been investigated in the context of turbulent hydrogen flames previously [8], in addition to its physical properties making it suitable for injection as a liquid. Therefore, if the experimental results indicate that toluene addition does not improve flame visibility at sufficiently low dopant concentrations, then other dopants are unlikely to be viable either. Toluene is also known to be formed as an intermediate species (along with other aromatic hydrocarbons) during the combustion of common biodiesel blends [22], so it can be considered a surrogate fuel to enable consistent experimental measurements in this sense. Note that in a practical implementation, it is unlikely that the use of toluene would be widespread, particularly in domestic settings.

Pure and toluene-doped hydrogen flames, in addition to natural gas flames, were analysed using a combination of flame photography and spectral imaging. Toluene vapour was produced via a controlled evaporator and mixing (CEM) unit, allowing a homogeneous mixture of hydrogen and toluene to be generated. Very low liquid flowrates of toluene into the CEM unit were achieved using a low-flow metering valve in conjunction with a Coriolis flow-meter, while the bulk gas flowrate was controlled with a thermal mass flow controller.

Flame photography was performed using a DSLR camera, operated with an exposure time of 0.2 s for the photographs presented in this report. The photographs were all captured with an f-number of 1.8 and an ISO value of 100, except where otherwise stated, with manual focus and white balance. The camera was also fitted with a notch filter centred at a wavelength of 594 nm with a FWHM of 23 nm. This was necessary to remove the effect of emissions from sodium excitation in the flame, as further discussed in Section 3.1. Unless otherwise stated, the flame photographs presented herein were captured with the notch filter fitted to the camera. In order to assess the visibility of the flames in different environments, photographs were captured with both an optically-absorbing (black velvet) background and a glossy white background, in both a dark and a well-lit room.

To further analyse the visible and infra-red emissions from the various flames, spectral imaging of the flames was performed using an Ocean Optics Red Tide USB650 spectrometer. This spectrometer was coupled to an optical fibre, which was in turn fitted to a collimating lens to increase the signal-to-noise ratio of the spectral data. These measurements provide a resolution to the nearest nm, with transmission ranging from the visible to near-IR region (approximately 400 – 850 nm). The flame spectra were collected under dark background conditions, and background noise corrections were also performed. A minimum of 30 spectral measurements were recorded for each flame case, which were then averaged to more clearly identify the peaks in the signal.

## 2.2 Burner configurations and boundary conditions

To study the effect of toluene addition under different scenarios, three different burner configurations were implemented in this investigation. A simple jet configuration was the initial focus, to simplify the analysis and enable future comparisons with numerical simulations. The burner was operated in non-premixed mode, with fuel issuing from an 8.0 mm I.D. jet into a coflow of room-temperature air. A single volumetric flowrate ( $\dot{V}$ ) of hydrogen was used, along with a natural gas case with equivalent heat input ( $Q_{in}$ ) for comparison. A range of toluene mass flowrates ( $\dot{m}_{tol}$ ) were also implemented, corresponding to a mole fraction ( $X_{tol}$ ) of toluene in the fuel mixture which ranged from 0–1%. The various flame cases for the simple jet configuration are shown in Table 1.

Table 1: Flame cases for 8-mm-diameter simple jet, including toluene mole fraction ( $X_{tol}$ ) as a percentage of the total fuel stream.

Case	$\dot{V}_{H_2}$ [SLPM]	$\dot{V}_{NG}$ [SLPM]	$\dot{m}_{tol}$ [mg/s]	$X_{tol}$ [%]	$Re_{jet}$	$Q_{in}$ [kW]
<b>JET-T0</b>	10	0	0	0.0	280	1.80
<b>JET-T1</b>	10	0	1.7	0.25	304	1.87
<b>JET-T2</b>	10	0	3.4	0.5	327	1.94
<b>JET-T3</b>	10	0	5.2	0.75	351	2.01
<b>JET-T4</b>	10	0	6.9	1.0	374	2.08
<b>JET-NG</b>	0	3.4	0	0	560	1.80

In addition to the simple jet flames, two typical domestic appliance burners were studied; namely a portable barbeque burner (GasMate) and a traditional gas stove-top burner (Bellini). These burners are designed to operate in premixed mode, using a passive air entrainment mechanism involving a fuel injection nozzle and air inlet regions. Due to the much higher flame speed of hydrogen and its propensity for flashback, the burners designed for natural gas had to be modified to prevent premixing from occurring when using hydrogen. Since it is of interest to compare the pure and doped hydrogen flames to the premixed natural gas flames for which these appliances are designed, data were collected for the premixed natural gas case prior to modifying the burners. The toluene concentration was again varied from 0–1% for both burners, and the hydrogen flowrates were assigned based on the rated heat input for the appliances. The boundary conditions and case names for the barbeque (BBQ) and stove (STV) burners are shown in Table 2.

Table 2: Flame cases for BBQ and STV burners, including toluene mole fraction ( $X_{tol}$ ) as a percentage of the total fuel stream.

Case	$\dot{V}_{H_2}$ [SLPM]	$\dot{V}_{NG}$ [SLPM]	$\dot{m}_{tol}$ [mg/s]	$X_{tol}$ [%]	$Q_{in}$ [kW]
BBQ-T0	8.5	0	0	0.0	1.53
BBQ-T1	8.5	0	2.0	0.35	1.61
BBQ-T2	8.5	0	2.9	0.5	1.65
BBQ-T4	8.5	0	5.9	0.75	1.71
BBQ-NG	0	2.9	0	0.0	1.53
STV-T0	9.1	0	0	0.0	1.64
STV-T1	9.1	0	1.6	0.25	1.70
STV-T2	9.1	0	3.1	0.5	1.76
STV-T4	9.1	0	6.3	0.75	1.83
STV-NG	0	3.2	0	0.0	1.64

### 3. RESULTS AND DISCUSSION

#### 3.1 Visible emissions from pure hydrogen flames

As mentioned in Section 1.2, it is often stated that pure hydrogen burns colourlessly and that the flames are “invisible”, although this is not strictly true. The primary source of visible emissions in pure hydrogen flames is from excited  $H_2O$  molecules, which produce a weak reddish appearance under certain conditions, along with a relatively weak blue continuum from reactions involving the OH and H radicals. During the current experiments, however, a bright orange colour was observed for the supposedly pure hydrogen flames. This has also been observed previously (see Section 1.2), and is often attributed to excitation of sodium, whose emission spectrum is dominated by the D-lines at 589.0 and 589.6 nm. To verify the source of the colour, spectral imaging of the “pure” hydrogen flames was performed. The spectral imaging showed a dominant peak at 589 nm, confirming the contribution of sodium excitation to the flame colour. An example of the  $H_2$  flame spectrum for the BBQ-T0 case is shown in Figure 1(a). The sodium peak at 589 nm is distinguishable, as are the peaks due to water vapour excitation in the infra-red region ( $\geq 700$ nm). Further spectra for selected  $H_2$ :NG blends ranging from 0% (pure NG) to 100% (pure  $H_2$ ) are later reported in Figure 5 and discussed in Section 3.3.

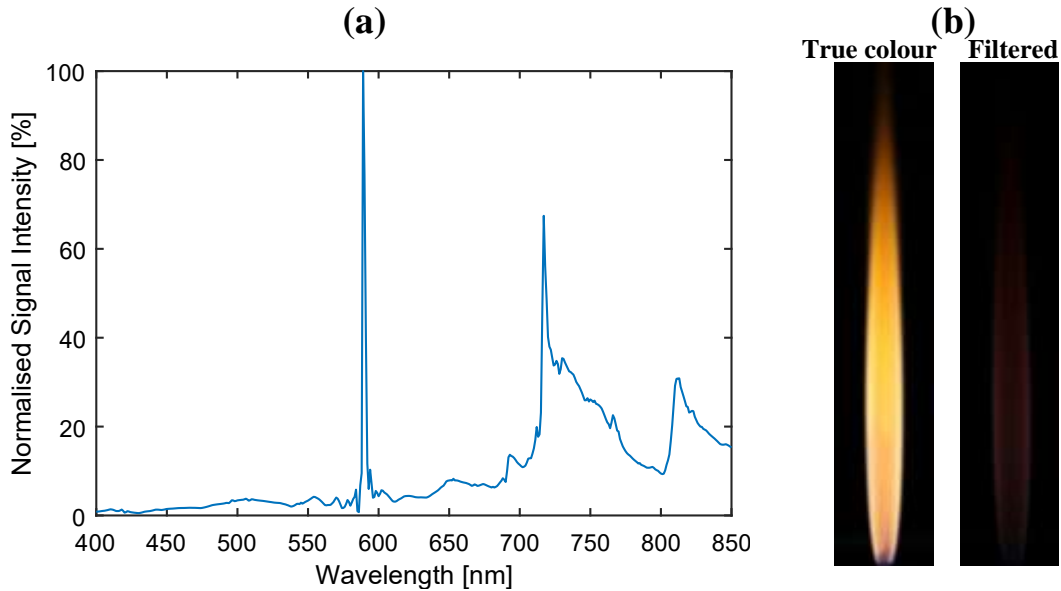


Figure 1: Effect of sodium impurity on hydrogen flame colour: (a) spectrum for BBQ-T0 case, and (b) photographs captured with and without the notch filter for the undoped jet flame (JET-T0).

The orange colour, in addition to the peak at 589 nm, was observed throughout the experiments with varying strength, including for the three different burner types. To identify the origin of the sodium, the plumbing system was purged with ethanol to ensure that it was not related to impurities within the pipes, with no effect observed. It was initially thought that the sodium could stem from the impurities within the hydrogen itself; however, no obvious difference was observed between industrial grade and ultra-high purity (Grade 5.0) hydrogen. Additionally, the D-lines due to sodium excitation were also observed for the spectra of natural gas flames in some cases; this is further explored in Section 3.3, which also presents results for blends of natural gas and hydrogen. This suggests that the source of sodium is in the air rather than the fuel, although it is possible that there was sodium present in both the hydrogen and the natural gas streams.

Since the presence of sodium is expected to change significantly depending on the surrounding environment, it cannot be consistently relied upon to produce a visible flame. As such, an optical filter was used for the flame photography to block out the light from sodium excitation, as described in Section 2.1. Figure 1(b) compares photographs captured with and without the filter on the camera for the simple jet configuration, highlighting the profound impact of the sodium emissions on the appearance of the flame. It should be noted that—due to the narrow blocking range of the filter—the use of this filter does not block out any other wavelengths of light which contribute to the colour of the flames other than those from the sodium lines. The remainder of the photographs presented in this report were captured with the notch filter attached.

### 3.2 Flame photography (with notch filter)

#### 3.2.1 Simple Jet Configuration

Photographs of the simple jet flames are shown in Figure 2, highlighting the change in appearance with addition of toluene. Toluene was added to hydrogen in four different concentrations up to 1% (by mole), with the equivalent heat input natural gas flame are also included in Figure 2 for comparison. The flame photography results show that addition of toluene does not significantly change the structure of the flames near the jet exit, although the effect further downstream is noticeable.

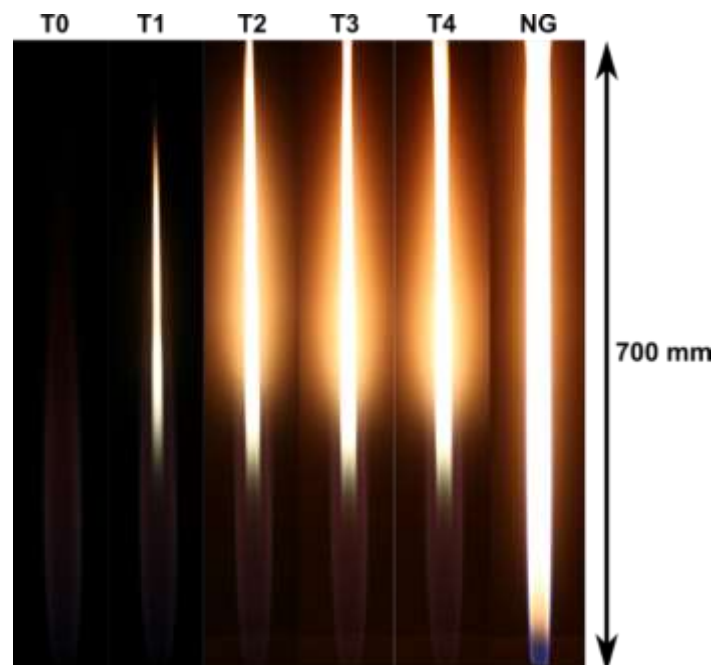


Figure 2: Photographs of simple jet flames with toluene addition from 0 – 1%, and equivalent natural gas flame (refer Table 2). All photographs captured with 1/5 sec exposure time.

For all of the flames with toluene, a luminous sooting region can be seen to form radially inwards from the main flame front. Interestingly, a similar study involving turbulent hydrogen-toluene flames diluted with nitrogen found that significant soot formation did not occur until the toluene concentration was increased to 3% per mole of  $H_2$  [8]. This difference is likely a result of the lack of turbulent mixing and longer residence times for the laminar flames in the current study, which increases the tendency for soot inception since precursor species are less likely to follow the oxidation pathway [23]. The luminous sooting region is relatively narrow for the 0.25% toluene case (T1), and the soot can be seen to be consumed within the frame of the photograph. There is a significant increase in intensity as the toluene concentration is increased to 0.5%, after which the effect of increasing toluene becomes less noticeable. From 0.5% to 1%, a broadening of the sooting region can be seen to occur, as well as a slightly further-upstream onset of soot formation. The sooting region is more uniformly distributed in the case of natural gas, with a reduced intensity from approximately 300 to 600 mm downstream of the jet exit in comparison to the cases with  $\geq 0.5\%$  toluene concentration.

### 3.2.2 BBQ Ring Burner Configuration

Similar to the simple jet flames, a range of toluene concentrations up to 1% by mole were investigated for the BBQ burner configuration. Photographs were captured with three different lighting/background conditions, to highlight the importance of these parameters when studying flame visibility. The different conditions are labelled as L0, L1 and L2, corresponding to lights off with a dark background (L0), lights on with a dark background (L1), and lights on with a white, glossy background (L2). The photography results are shown in Figure 3(a), for toluene concentrations of 0 (i.e. pure hydrogen), 0.5% and 1%, all operated in nonpremixed mode, while the equivalent natural gas flame shown is premixed. In order to avoid saturation of the images under the L2 condition, the f-number of the camera was increased from 1.8 to 5 for these photographs.

In Figure 3(a), a significant change in the appearance of the flames can again be seen with addition of toluene due to soot formation. Albeit weak, the pure hydrogen flame can be just made out under the “lights off” conditions (top-left frame, column “L0”), with a faint blue region near the burner and a reddish appearance further downstream. With the lights turned on the flame becomes much more difficult to observe; a very faint flame can be seen with the dark background (L1) while the flame appears invisible with the white, glossy background (L2), which simulates a kitchen environment. At 0.5% toluene (T2) there is a luminous sooting region enclosed within the outer structure, which can be clearly seen under the L0 and L1 conditions, while it is much less apparent under the L2 conditions. There is a significant increase in soot formation as the toluene concentration is increased from 0.5% to 1%, with the flame being clearly visible for all three conditions. The difference between the BBQ-T2 and BBQ-T4 flames is an interesting departure from the observations relating to the simple jet configuration, in which the increase from 0.5% to 1% did not have a major impact on the luminosity. This difference is likely a result of the change in the flow-field and mixing processes between the two types of burners. In particular, the ring burner features a number of narrow ports from which the fuel issues, leading to a more complex mixing field and a potential change in soot formation mechanisms. The premixed natural gas flame can also be observed under all three lighting conditions shown in Figure 3(a). It is worth pointing out, however, that under the L2 conditions, the blue natural gas flame can only be seen against the dark backdrop of the burner body, and is very difficult to distinguish against the white background. These results emphasise the importance of considering the surroundings when evaluating the visibility and safety of flames for domestic applications.

The length of the flames also increases significantly with toluene addition, particularly from the BBQ-T2 to the BBQ-T4 case. It is interesting to note that the pure hydrogen flame displays a similar shape and flame length to the equivalent premixed natural gas flame, despite operating in nonpremixed mode. This suggests that it could be feasible to simply modify these types of burners to prevent premixing to allow them to run on 100%  $H_2$  in practice, although if toluene (or a similar sooting fuel) were to be added then it would need to be appropriately designed in order to prevent flame impingement on the surface being heated.

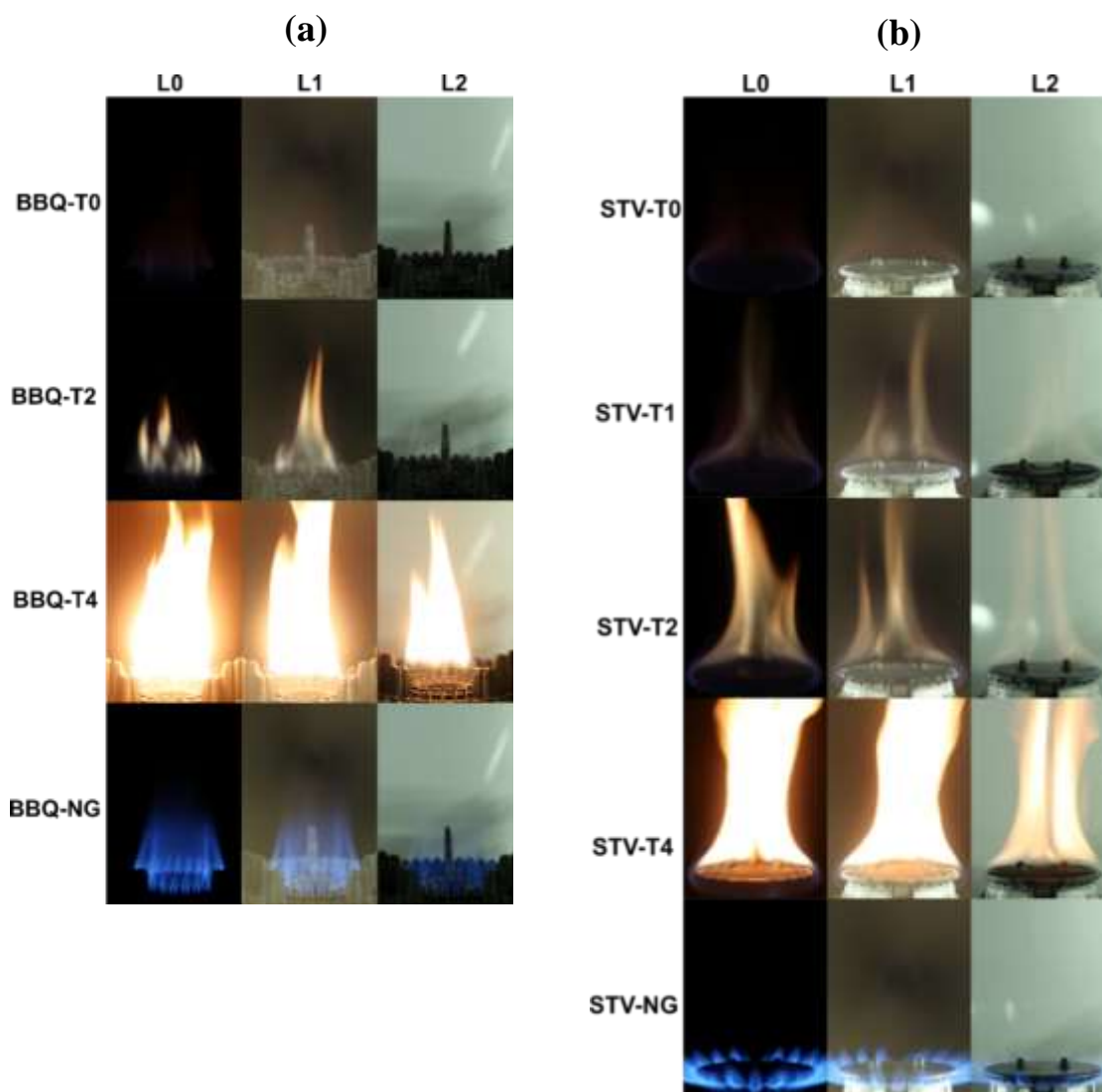


Figure 3: Photographs of (a) the “BBQ” flames and (b) the “STV” flames (refer Table 2) under different lighting and background conditions. Images were captured with 1/5 sec exposure time, with an f-number of 1.8 for L0 and L1 conditions (dark background with lights off and on, respectively) and f-number of 5 for the L2 condition (lights on with white background).

### 3.2.3 Stove-top Burner Configuration

Photographs of the flames under the three different lighting/background conditions are shown for the stove-top burner in Figure 3(b). Once again, the photographs corresponding to the L2 condition were captured with an f-number of 5 instead of 1.8 to prevent saturation of the images. For this burner, results are shown for toluene concentrations of 0, 0.25%, 0.5% and 1%, along with the equivalent heat input premixed natural gas flame. Once again, the pure hydrogen flame is visible under the L0 and L1 conditions, and virtually undetectable with the L2 background. There is again a noticeable increase in soot formation and therefore luminosity as the toluene is added, with the STV-T1 flame displaying a faint sooting region which can be observed under all three conditions, although it is very faint under the L2 condition. Similar to the BBQ burner, the effect of increasing from 0.5 to 1% toluene is significant, with the incandescence from the soot dominating the appearance of the flame for the STV-T4 flame. The natural gas flame can again be seen under all three conditions, although detection against the white background is difficult. These results indicate that addition of toluene at  $\geq 0.25\%$  can produce a flame that is of similar or improved visibility to that of natural gas.



Comparing the hydrogen/toluene flames with the equivalent natural gas flame in Figure 3(b), it is evident that the lack of premixing leads to a significant change in the shape and length of the flames. While for the BBQ burner in Figure 3(a) the pure hydrogen flame showed a similar behaviour to the natural gas flame, this is not the case for the stove burner. While the premixed natural gas flame features distinct flamelets which branch outwards from the exit ports, the hydrogen case appears to be stabilised as a single flame with its base below the exit ports and a large “tail” which extends downstream. The flame length then increases significantly with addition of toluene, similar to the observations for the previous burners. This suggests that this type of burner would need to be operated in either premixed or partially-premixed mode, or modifications to the burner geometry would be necessary to enable efficient and safe use with hydrogen as the dominant fuel source if operated in nonpremixed mode. It is also worth noting that these changes would also lead to changes in visibility which would require further investigation.

### 3.3 Spectral measurements of natural gas/hydrogen flames

As mentioned in Section 3.1, the emission of light due to the excitation of sodium within the hydrogen flames was found to be significant during these experiments. Since the presence of sodium did not appear to change noticeably when using both industrial grade and ultra-high purity hydrogen—nor after purging the piping system—it was hypothesised that the sodium instead stems from the surrounding air. While there is limited data available regarding the presence of sodium in ambient air, it is known to be one of several sources of particulate matter, occurring both naturally from suspended sea salt and due to anthropogenic sources [24]. It is worth mentioning that the current experiments were conducted in relatively close proximity to the ocean within the City of Adelaide, such that both sources of sodium are likely to be significant.

Although the emission of light due to sodium excitation was noticeable for the hydrogen flames, it is interesting to note that this behaviour was not apparent for the natural gas flames, at least based upon qualitative observations by eye. Therefore, spectrometer measurements were performed to determine if this feature was unique to the hydrogen flames. These results are shown for the three different burners operating on natural gas in Figure 4.

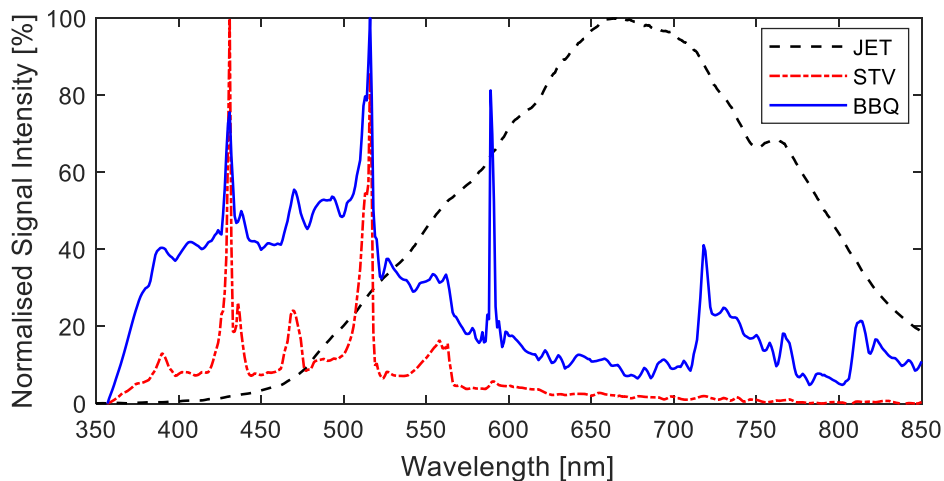


Figure 4: Flame spectra for natural gas flames for the three different burner configurations, for wavelengths ranging from near-UV to near-IR. Note that “JET” case is non-premixed, while “STV” and “BBQ” are premixed.

From Figure 4, it is apparent that the flame emission spectrum is sensitive to the burner configuration that is implemented. First of all, it is important to note that the “JET” spectrum shown corresponds to a non-premixed flame, such that soot formation is significant, as shown in the photograph of this flame in Figure 2. As a result, the spectrum is dominated by black-body radiation due to the high-temperature soot particles, and there is minimal radiation in the 350–450 nm range. The premixed burners, as expected, do not display this broadband radiation, instead showing peaks in the “near-UV/blue” region

(i.e. approximately 350–500 nm), which are well-characterised for hydrocarbon flames and correspond primarily to  $\text{CH}^*$  radicals and the  $\text{C}_2$  Swan bands [11]. Importantly, it can be seen from the “BBQ” spectrum that there are indeed emissions from excited sodium for this case, with the characteristic peak at 589 nm, similar to the  $\text{H}_2$  spectrum shown in Figure 1. There is also a very slight peak in the spectrum of the “STV” flame at 589 nm, although it is much less intense in comparison to the BBQ case and difficult to distinguish in Figure 4. It is also interesting to observe that the BBQ flame displays peaks in the red/near-IR region which are characteristic of excitation of water molecules, similar to the spectrum of the equivalent  $\text{H}_2$  flame, while this behaviour is not apparent for the stove-top burner.

To further explore the source of the sodium emissions, results from a separate set of spectral measurements involving blends of  $\text{H}_2$  and natural gas (NG) have been analysed. This series of experiments involved flame cases ranging from pure  $\text{H}_2$  to pure NG, with eight intermediate NG: $\text{H}_2$  ratios. A stove-top burner configuration was used for these experiments, similar to the STV burner, although the burner was operated in premixed mode without modification for all flame cases. As a result, the flames transitioned from a conventional stove-top behaviour for low-to-intermediate  $\text{H}_2$  concentrations, with flamelets stabilised at the exit ports between the burner crown and the cap, to a “light-back” condition in which the flame burns inside the mixing region, that is, between the fuel injector and the exit ports. Based on qualitative observations, this light-back situation occurred for  $\text{H}_2$  concentrations of 80% (by volume) and greater. The spectral imaging results are shown in Figure 5, for a selection of cases shown on a single set of axes, for two different wavelength ranges; specifically, from 350–550 nm and from 580–600 nm, to highlight specific features of the spectra.

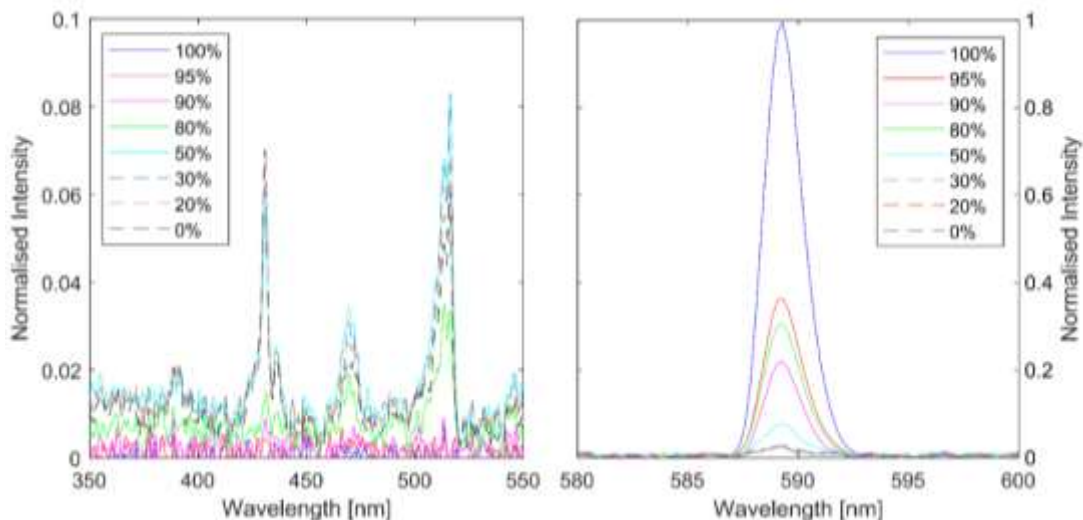


Figure 5: Measured spectra for selected  $\text{H}_2$ :NG blends from 0% (pure NG) to 100% (pure  $\text{H}_2$ ). Results are shown for two different wavelength ranges to focus on the “blue” region (left) and the sodium emissions (right). Values in legend are the percentage of  $\text{H}_2$  in the fuel.

A noticeable change in the spectra of the various blends can be seen for both wavelength ranges shown in Figure 5. The 580–600 nm plots focus on peaks at 589 nm (sodium excitation). It is interesting to note the rapid reduction in the intensity of this “sodium peak” as the  $\text{H}_2$  concentration is decreased from 100%, even with just 5% NG by volume (that is, the 95% case). While the NG-dominated cases show a greatly diminished peak at this location, the peak remains present for all cases, and there does not appear to be any noticeable change from 30%  $\text{H}_2$  case to the pure NG case.

The fact that there is still a slight peak for the NG-dominated flames—coupled with the strong peak observed for the BBQ-NG case (see Figure 4)—indicates that the primary source of the sodium is not from the hydrogen itself. The effect seen in Figure 5 must therefore be related to a change in flame behaviour as hydrogen is added to natural gas. One factor which likely contributes to this change is the transition from a conventional cooktop flame for the flames with 50%  $\text{H}_2$  and less, to a flame which is lit-back for  $\text{H}_2$  concentrations of 80% and greater; this would explain the relatively large increase from 50% to 80%  $\text{H}_2$ . This is also consistent with the spectra from 350–550 nm shown in Figure 5, in which

the  $\leq 50\%$   $H_2$  cases can all be seen to have very similar spectra both in terms of the location of the peaks and their intensities. It should also be noted that these peaks which can be seen in the 350–550 nm range in Figure 5 correspond to the well-characterised emission bands for hydrocarbon flames which are also evident for the STV and BBQ burner spectra shown in Figure 4.

While the light-back effect under sufficiently high  $H_2$  concentrations appears to have an effect on the flame spectrum, this does not completely explain the observations regarding the peak at approximately 589 nm. If the flame being lit-back were the sole cause, then one would not expect the increase in intensity which occurs from 90% to 100%  $H_2$  as shown in Figure 5, nor would it explain the detection of sodium emissions for the simple jet configuration and the BBQ burner, for both nonpremixed hydrogen and premixed natural gas in the case of the BBQ burner. Based on these results, it is likely that there are multiple factors which affect the emission of light at 589 nm. Since the behaviour is observed across different burner configurations and plumbing systems, it follows that the sodium either stems from the surrounding air, or it is present in both the natural gas (from the mains network) and the hydrogen (from a cylinder). In addition to the source, the actual mechanism which leads to the sodium excitation and emission of light is not clear. While temperature measurements were not performed in this study, an increase in the  $H_2$  concentration is expected to lead to a slightly hotter flame, which could lead to an increased tendency for excitation to occur. However, the temperature difference between the 99% and 100%  $H_2$  flames is insignificant, yet there is a relatively large increase in intensity. Additionally, the premixed BBQ-NG case was seen to have a strong emission at 589 nm, as well as peaks in the red/near-IR region of the spectrum which align to those observed for the equivalent  $H_2$  flame and are attributed to excitation of water molecules. This suggests a change in behaviour for the premixed BBQ burner in comparison to the stove-top burner, which is likely a result of a change in the entrainment of air and mixing processes. This could in turn lead to a change in temperature and/or oxidation pathways, such that excitation of sodium and water are favoured in the case of the BBQ burner, although this requires further investigation.

#### 4. CONCLUSIONS

The use of 100% hydrogen as a fuel for domestic heating applications presents a number of challenges in terms of both safety and performance. Many of these challenges are related to the difference in combustion behaviour of hydrogen in comparison to natural gas. It is well-documented that hydrogen burns with a relatively faint flame due to a lack of soot and carbon-containing species, such that it is often described as being invisible under regular lighting conditions; this presents an obvious safety concern for applications such as cooktop burners. An investigation has therefore been carried out to assess the feasibility of improving flame visibility through the addition of a highly sooting fuel, with the focus on toluene as a surrogate fuel for this project. There are also potential side-benefits of the addition of such a fuel, in terms of leak detection via olfactory sensation and increased thermal radiation.

A review of the relevant literature revealed a number of interesting findings with regards to the visible emissions associated with hydrogen flames. An interesting observation was the apparent lack of consensus across different studies, particularly with regards to the “reddish” appearance of hydrogen flames and the effect of impurities. An experimental study was performed to examine the behaviour of toluene-doped hydrogen flames for three different burner configurations. The flames were analysed via photography under various lighting and background conditions, complemented by spectral imaging. A particularly interesting finding was the dominance of the visible emissions from sodium impurities on the visual appearance of the pure hydrogen flames, which necessitated the use of a notch filter for the flame photography to capture the visible emissions from the underlying hydrogen flame. Spectral imaging revealed that emissions due to the presence of sodium also occurred for natural gas under certain configurations, although increasing the concentration of hydrogen in the fuel tends to promote sodium excitation. The addition of toluene up to 1% by mole was found to have a significant impact on the visual appearance of the flames, as well as the radiative heat flux. For the two practical burners, photographs were captured under a range of background/lighting conditions which were found to have a notable effect on the visibility, emphasising the importance of these parameters when analysing the safety of flames in domestic applications.

## 5. ACKNOWLEDGEMENTS

The authors acknowledge the generous financial support from the Australian Research Council (ARC) and the Future Fuels Cooperative Research Centre (FF-CRC).

## 6. REFERENCES

1. G.W. Crabtree, M.S. Dresselhaus, and M.V. Buchanan, The Hydrogen Economy, *Physics Today*, **57**, No. 12, 2004, p. 39-44.
2. P.E. Dodds, et al., Hydrogen and Fuel Cell Technologies for Heating: A Review, *International Journal of Hydrogen Energy*, **40**, No. 5, 2015, p. 2065-2083.
3. C.M. White, R.R. Steeper, and A.E. Lutz, The Hydrogen-Fueled Internal Combustion Engine: A Technical Review, *International Journal of Hydrogen Energy*, **31**, No. 10, 2006, p. 1292-1305.
4. M.W. Melaina, O. Antonia, and M. Penev, *Blending Hydrogen into Natural Gas Pipeline Networks: A Review of Key Issues*. 2013, NREL.
5. R. Judd and D. Pinchbeck, *Hydrogen admixture to the natural gas grid*, in *Compendium of Hydrogen Energy*. 2016. p. 165-192.
6. R.W. Schefer, et al., Visible emission of hydrogen flames, *Combustion and Flame*, **156**, No. 6, 2009, p. 1234-1241.
7. DNV, *Hydrogen Colourant - Final Report*. 2019, Hy4Heat.
8. M.J. Evans, et al., Highly radiating hydrogen flames: Effect of toluene concentration and phase, *Proceedings of the Combustion Institute*, **38**, No. 1, 2021, p. 1099-1106.
9. A.J. Gee, et al., Toluene addition to turbulent H<sub>2</sub>/natural gas flames in bluff-body burners, *International Journal of Hydrogen Energy*, **47**, No. 65, 2022, p. 27733-27746.
10. M. Zarzo, Effect of functional group and carbon chain length on the odor detection threshold of aliphatic compounds, *Sensors*, **12**, No. 4, 2012, p. 4105-12.
11. A. Gaydon, *The Spectroscopy of Flames*. 1974: Springer Netherlands.
12. Y. Zhao, et al., Investigation of visible light emission from hydrogen-air research flames, *International Journal of Hydrogen Energy*, **44**, No. 39, 2019, p. 22347-22354.
13. A. Choudhuri, Combustion characteristics of hydrogen–hydrocarbon hybrid fuels, *International Journal of Hydrogen Energy*, **25**, No. 5, 2000, p. 451-462.
14. P.J. Padley, The origin of the blue continuum in the hydrogen flame, *Transactions of the Faraday Society*, **56**, No., 1960.
15. H.A. Webster, Visible Spectra of Standard Navy Colored Flares, *Propellants, Explosives, Pyrotechnics*, **10**, No. 1, 1985, p. 1-4.
16. D. Juknelevicius, et al., A Spectrophotometric Study of Red Pyrotechnic Flame Properties Using Three Classical Oxidizers: Ammonium Perchlorate, Potassium Perchlorate, Potassium Chlorate, *Zeitschrift für anorganische und allgemeine Chemie*, **640**, No. 12-13, 2014, p. 2560-2565.
17. K. Waheed, et al., Investigations on Thermal Radiative Characteristics of LPG Combustion: Effect of Alumina Nanoparticles Addition, *Combustion Science and Technology*, **187**, No. 6, 2014, p. 827-842.
18. AEMO, *Gas Quality Guidelines*. 2017, Australian Energy Market Operator.
19. W. Hutny and G. Lee, Improved radiative heat transfer from hydrogen flames, *International Journal of Hydrogen Energy*, **16**, No. 1, 1991, p. 47-53.
20. C. McEnally and L. Pfefferle, Improved sooting tendency measurements for aromatic hydrocarbons and their implications for naphthalene formation pathways, *Combustion and Flame*, **148**, No. 4, 2007, p. 210-222.
21. P. Chylek, S.G. Jennings, and R. Pinnick, *SOOT*, in *Encyclopedia of Atmospheric Sciences*, J.R. Holton, Editor. 2003, Academic Press: Oxford. p. 2093-2099.
22. H.Y. Kim and N.J. Choi, Study on Volatile Organic Compounds from Diesel Engine Fueled with Palm Oil Biodiesel Blends at Low Idle Speed, *Applied Sciences*, **10**, No. 14, 2020.
23. S.M. Mahmoud, et al., The effect of exit Reynolds number on soot volume fraction in turbulent non-premixed jet flames, *Combustion and Flame*, **187**, No., 2018, p. 42-51.
24. A. Ooki, et al., Sources of sodium in atmospheric fine particles, *Atmospheric Environment*, **36**, No. 27, 2002, p. 4367-4374.